

**DEVELOPMENT OF A COTS RADIODETECTOR SYSTEM USING PHOSWICH DETECTORS  
AND PULSE SHAPE ANALYSIS**

Wolfgang Hennig<sup>1</sup>, Hui Tan<sup>1</sup>, William K. Warburton<sup>1</sup>, Anthony Fallu-Labruyere<sup>1</sup>, Konstantin Sabourov<sup>1</sup>,  
Matthew W. Cooper<sup>2</sup>, Justin I. McIntyre<sup>2</sup>, and Anshel Gleyzer<sup>3</sup>

XIA LLC<sup>1</sup>, Pacific Northwest National Laboratory<sup>2</sup>, and PhotoPeak, Inc<sup>3</sup>

Sponsored by National Nuclear Security Administration

Contract No. DE-FG02-04ER84121

**ABSTRACT**

Several of the radioxenon detection systems developed for the International Monitoring System use beta/gamma coincidence detection to achieve high sensitivity. These systems, e.g., the Automated Radioxenon Sampler and Analyzer (ARSA) or the Swedish Automatic Unit for Noble gas Acquisition (SAUNA), currently use an arrangement of separate beta and gamma detectors to detect beta/gamma coincidence events characteristic of the different radioxenon isotopes. While they are very sensitive to small amounts of radioxenon, they also require careful calibration and gain matching of several detectors and photomultiplier tubes. An alternative approach is the use of a single phoswich detector in which beta-gamma coincidences are detected by pulse shape analysis (PSA). We previously reported the development of prototype phoswich well detectors, consisting of a fast plastic scintillator (absorbing betas) optically coupled to a slower CsI(Tl) scintillator (absorbing gammas). These detectors thus require only a single photomultiplier tube and an electronics readout channel. Beta/gamma coincidences create characteristic “fast/slow” signals that can easily be distinguished from “slow only” or “fast only” non-coincident interactions.

In this paper, we will describe the development of a commercial off-the-shelf (COTS) radioxenon detector system based on such phoswich detectors. The PSA functions were implemented using the digital signal processor in a set of commercial readout electronics that is also compatible with ARSA and SAUNA detectors. These functions detect coincidences in real time and accumulate 2D histograms in on-board memory. The acquisition and the PSA functions are operated through a C driver library that is called from a graphical user interface but can also be integrated into larger-scale acquisition and control software. Several phoswich detectors have been manufactured in a small-scale production run, and have been characterized for energy resolution, separation of coincidence events in 2D beta/gamma energy histograms, and detection efficiency using a variety of test sources, and for background count rates. In addition, a test pulser module has been developed to support monitoring and testing of the electronics for state of health during operation. The phoswich detector, readout electronics, and software are now available as a COTS product package (“PhosWatch”) that is currently being beta-tested at several radioxenon monitoring research laboratories.

<b>Report Documentation Page</b>			Form Approved OMB No. 0704-0188	
<p>Public reporting burden for the collection of information is estimated to average 1 hour per response, including the time for reviewing instructions, searching existing data sources, gathering and maintaining the data needed, and completing and reviewing the collection of information. Send comments regarding this burden estimate or any other aspect of this collection of information, including suggestions for reducing this burden, to Washington Headquarters Services, Directorate for Information Operations and Reports, 1215 Jefferson Davis Highway, Suite 1204, Arlington VA 22202-4302. Respondents should be aware that notwithstanding any other provision of law, no person shall be subject to a penalty for failing to comply with a collection of information if it does not display a currently valid OMB control number.</p>				
1. REPORT DATE <b>SEP 2008</b>	2. REPORT TYPE	3. DATES COVERED <b>00-00-2007 to 00-00-2007</b>		
<b>4. TITLE AND SUBTITLE</b> <b>Development of a COTS Radioxenon Detector System Using Phoswich Detectors and Pulse Shape Analysis</b>			5a. CONTRACT NUMBER	
			5b. GRANT NUMBER	
			5c. PROGRAM ELEMENT NUMBER	
<b>6. AUTHOR(S)</b>			5d. PROJECT NUMBER	
			5e. TASK NUMBER	
			5f. WORK UNIT NUMBER	
<b>7. PERFORMING ORGANIZATION NAME(S) AND ADDRESS(ES)</b> <b>Pacific Northwest National Laboratory, PO Box 999, Richland, WA, 99352</b>			8. PERFORMING ORGANIZATION REPORT NUMBER	
<b>9. SPONSORING/MONITORING AGENCY NAME(S) AND ADDRESS(ES)</b>			10. SPONSOR/MONITOR'S ACRONYM(S)	
			11. SPONSOR/MONITOR'S REPORT NUMBER(S)	
<b>12. DISTRIBUTION/AVAILABILITY STATEMENT</b> <b>Approved for public release; distribution unlimited</b>				
<b>13. SUPPLEMENTARY NOTES</b> <b>Proceedings of the 30th Monitoring Research Review: Ground-Based Nuclear Explosion Monitoring Technologies, 23-25 Sep 2008, Portsmouth, VA sponsored by the National Nuclear Security Administration (NNSA) and the Air Force Research Laboratory (AFRL)</b>				
<b>14. ABSTRACT</b> <b>see report</b>				
<b>15. SUBJECT TERMS</b>				
<b>16. SECURITY CLASSIFICATION OF:</b> a. REPORT      b. ABSTRACT      c. THIS PAGE <b>unclassified</b> <b>unclassified</b> <b>unclassified</b>			<b>17. LIMITATION OF ABSTRACT</b> <b>Same as Report (SAR)</b>	<b>18. NUMBER OF PAGES</b> <b>10</b>
<b>19a. NAME OF RESPONSIBLE PERSON</b>				

## **OBJECTIVES**

Systems to measure the amount of radioactive xenon in the atmosphere, part of the International Monitoring System established by the Comprehensive Nuclear-Test-Ban Treaty to detect nuclear weapons testing, have been installed in several locations around the world. Several of these radioxenon detection systems, e.g., the ARSA or the SAUNA, use beta/gamma coincidence detection to suppress non-coincident background and achieve high sensitivity to the coincidence events characteristic of the radioxenon isotopes of interest (Reeder, 1998; Ringbom et al., 2003).

While these systems are very sensitive to small amounts of radioxenon, their complex arrangement of separate beta and gamma detectors also requires careful calibration and gain matching, which can make them cumbersome to operate. An alternative approach is the use of a single phoswich detector (Ely, 2003; Hennig, 2006-1; Farsoni et al., 2007) in which beta/gamma coincidences are detected by PSA. We previously reported the development of prototype phoswich well detectors (Hennig, 2007-1), consisting of a fast plastic scintillator cell containing the Xe gas and mainly absorbing beta particles and conversion electrons, optically coupled to and surrounded by a slower CsI(Tl) scintillator mainly absorbing X-rays and gamma rays. The phoswich detector thus requires only a single photomultiplier tube (PMT) and electronics readout channel. Beta/gamma coincidences create characteristic “fast/slow” signals that can easily be distinguished from “slow only” or “fast only” non-coincident interactions by PSA algorithms.

The objective of the work presented in this paper is to develop a COTS radioxenon detector unit based on phoswich detectors that can be used as a drop-in replacement for ARSA or SAUNA detector units. This objective consists of several tasks: 1) Manufacturing phoswich detectors in a small-scale production run and characterizing their performance. 2) Implementing the PSA functions in the digital signal processor (DSP) of the readout electronics (the DGF Pixie-4; Hennig, 2007-2) and integrating control of and output from PSA functions into the Pixie-4 user interface. 3) Developing a programmable coincidence pulse generator (“pulser”) to support monitoring and testing of the electronics for state of health during operation. The research accomplished in each of these three tasks is described below.

## **RESEARCH ACCOMPLISHED**

### **Detector Production and Characterization**

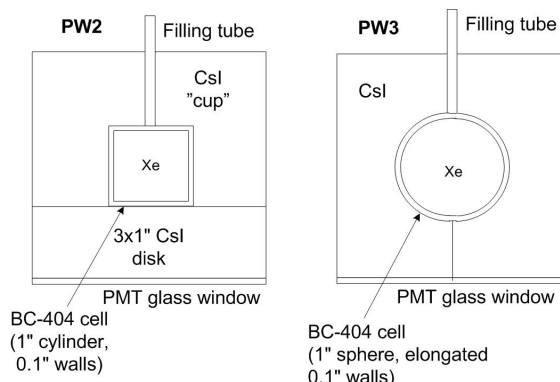


**Figure 1. Geometries of phoswich well detectors studied. Left: 1st well prototype (PW2). Right: 2nd well prototype and production detectors (PW3-PW7).**

At the time of this writing, a total of six phoswich well detectors have been built, named PW2-PW7. They all consist of a 1"-diameter BC-404 plastic cell enclosed in and optically coupled to a 3"-diameter CsI(Tl) crystal, but differ in detector geometry as shown in Figure 1. The geometry of the first well detector prototype PW2 is easier to manufacture, but due to the cut in CsI parallel to the PMT window, the light collection and thus energy resolution are degraded according to simulations (Hennig, 2006-2). The geometry of PW3-PW7, an elongated spherical cell embedded in a CsI crystal cut perpendicular to the PMT window, has the best light collection and resolution among all designs studied in simulations, though it is more difficult to manufacture. PW2, PW4, and PW5 use PMT model 9305KB (Electron Tubes, Inc), PW6-PW7 use PMT model R1307 (Hamamatsu). PW3 originally used PMT model

9305KB, but since this particular PMT performed poorly (low gain and noisy), PW3 was rebuilt with a new PMT and crystal and renamed to PW3a.

For each detector, acquisition parameters such as gain, HV bias, trigger thresholds and energy filter settings were first individually optimized for best performance. Detectors were then characterized by measuring resolutions at various energies with a number of test sources (see Table 1). It can be seen that PW2 achieves good resolutions at low energies, but at higher energies the resolutions degrade and the spectrum even shows double peaks. We attribute this to the different light-collection efficiency in the two sections of the CsI crystal, resulting in an estimated ~6% higher PMT signal amplitude from photons absorbed in the lower section of the CsI crystal than from photons absorbed in the upper section (Hennig, 2006-2). This amplitude difference adds in quadrature to other peak broadening effects (e.g., photostatistics), and thus becomes negligible at low energies, but not at high energies. PW3, the second prototype, achieved good resolution at high energies (~9% full width at half maximum [FWHM] at 662 keV), but with the original low gain, noisy PMT achieved only ~47% at 30 keV from  $^{133}\text{Xe}$  (small signal close to noise). PW4 and PW5, having preselected the PMT before assembly, combine the good resolution at high energy due to the better crystal geometry with the good resolution at low energy due to the low-noise PMT. PW6, PW7, and PW3a, using a different PMT and biasing system with even lower noise, achieve the best energy resolution of all detectors studied, except for low-energy beta lines.

**Table 1. Energy resolution (FWHM) for various energies. Measurements with external sources use no PSA and measure only the energy deposited in CsI (Ec). Measurements with internal sources use PSA to extract the energy deposited in CsI by gamma-only events (Eco), the energy deposited in the plastic scintillator by beta-only events (Epb), and the energies deposited in either scintillator in coincidence events (Ecb and Epc). Numbers in () indicate non-optimal measurements as explained in the notes. Measurements with the rebuilt detector PW3a are still in progress.**

Resolution (FWHM)	PW2	PW3a	PW4	PW5	PW6	PW7	Notes
PMT model	9305KB	R1307	9305KB	9305KB	R1307	R1307	
Ec = 662keV (external $^{137}\text{Cs}$ )	(12%)	7.0%	8.4%	8.5%	7.3%	7.2%	PW2: two peaks, ~7% and ~9%
Ec = 120keV (external $^{57}\text{Co}$ )	16%	11.4%	13%	14%	12.7%	11.6%	
Ec = 60keV	18%	16%	17%	19%	17%	16%	
Ec = 26keV (external $^{241}\text{Am}$ )	31%	28%	34%	32%	29%	27%	
Ecb = 20keV	39%	(28%)	--	--	34%	32%	PW3a: preliminary
Eco = 88 keV	19%	(20%)	--	--	17%	16%	
Epb = 60 keV	44%				50%	47%	
Epo = 88 keV (internal $^{109}\text{Cd}$ )	33%				43%	58%	
Ecb = 609keV (internal $^{222}\text{Rn}$ )	(12%)		--	--	--	7.8%	PW2: two peaks, ~7% and ~9%
Ecb = 80keV (internal $^{133}\text{Xe}$ )	20%		21%	21%	17%	16%	
Ecb = 30keV	35%		35%	34%	30%	28%	
Epb = 129keV	26%		--	29%	33%	33%	
Epo = 160 keV (internal $^{131m/133}\text{Xe}$ )	29%		--	29%	33%	34%	

The photon energy resolutions of the “production detectors” PW4-PW7 are significantly better than resolutions reported for the ARSA detector, which achieves ~12% (FWHM) at 662 keV (Reeder, 2004) compared to ~8.5% for PW4 and PW5 and even 7.3-7.0% for PW6, PW7, and PW3a. For energies above 80 keV, the production detectors also match or exceed the resolutions obtained with Pacific Northwest National Laboratory's (PNNL's) redesigned  $\beta-\gamma$  detector, which in the preferred CsI(Na) variant achieves ~8.7% at 662 keV (Cooper, 2007-1). PW6, PW7, and PW3a even match or exceed the resolution of the SAUNA II detector, which achieves ~7.3% at 662 keV. However,

when comparing these resolutions it should be kept in mind that count rates and other experimental conditions can not be assumed to be the same for measurements performed at different times and institutions.

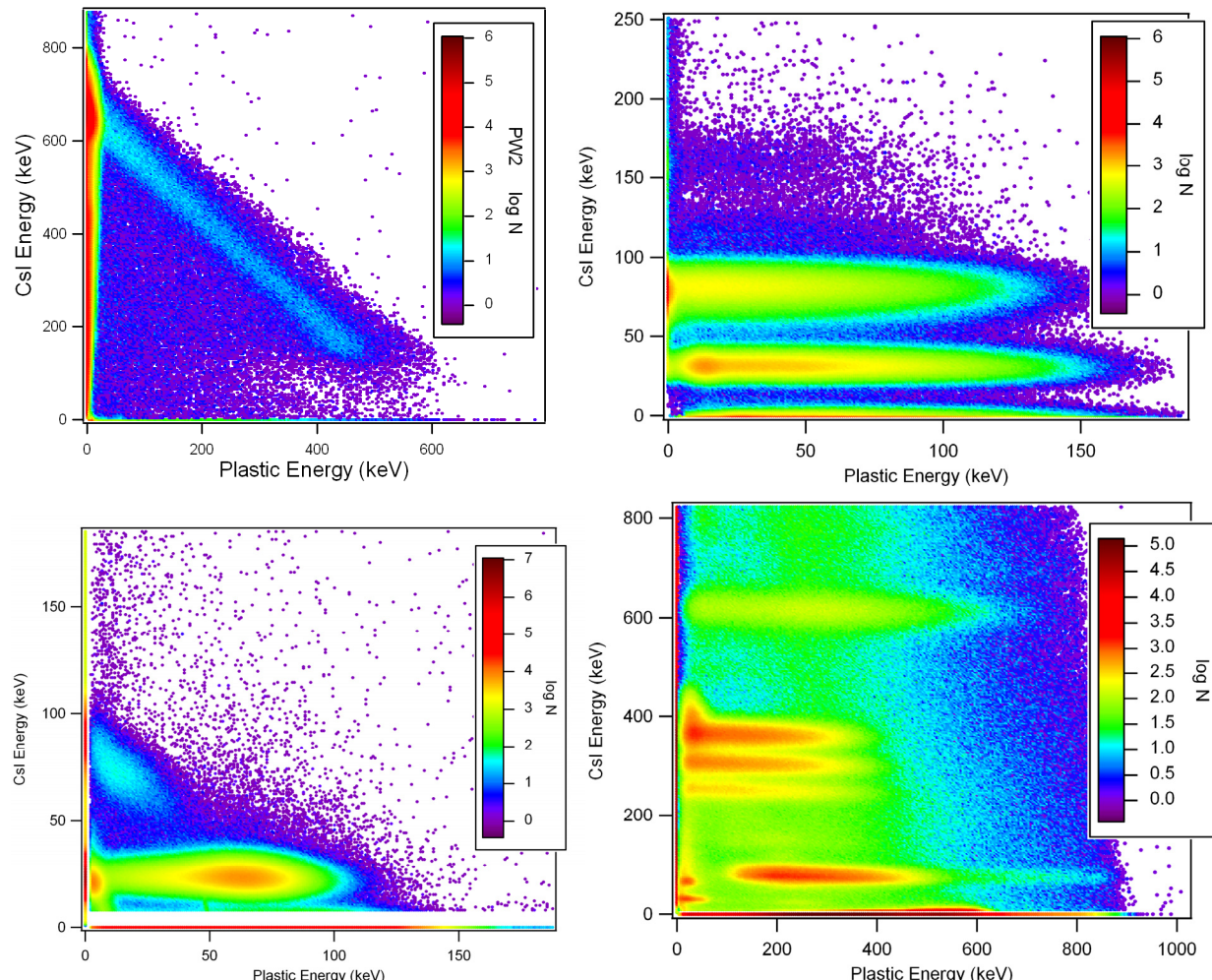


**Figure 2. 2D energy histograms from PW2 for a  $^{137}\text{Cs}$  source (upper left), from PW5 for a  $^{133}\text{Xe}$  source (upper right), from PW2 for a  $^{109}\text{Cd}$  source (lower left), and from PW7 for a  $^{222}\text{Rn}$  source with some residual  $^{133}\text{Ba}$  (lower right). In the lower spectra, non-coincident events have been contracted to the axes.**

Typical 2D histograms plotting the energy deposited in CsI (Ec) vs. the energy deposited in the plastic scintillator (Ep) are shown in Figure 2 for a variety of sources. Several issues are worth noting:

- All detectors achieve excellent linearity in the 2D spectrum, as indicated by the straight line of the  $^{137}\text{Cs}$  Compton scatter events. In contrast, some curvature can be observed in most ARSA or SAUNA 2D histograms, indicating non-linear effects in the energy measurement, e.g., due to PMT gain variations with deposited energy.
- The  $^{109}\text{Cd}$  measurements were performed with the source material deposited on a thin rod, inserted into the detector through the filling tube. Having similar decay energies and decay modes than  $^{131\text{m}}\text{Xe}$ ,  $^{109}\text{Cd}$  can substitute for  $^{131\text{m}}\text{Xe}$  in test and calibration measurement. Since it is a solid source with a long decay time, it is much easier to handle. In addition, it has the advantage that repeated measurements are more consistent, since the amount of  $^{109}\text{Cd}$  in the source is the same in each measurement (except for the decay, which can be computed), whereas knowing the exact amount of  $^{131\text{m}}\text{Xe}$  in a test measurement is not trivial.

- In  $^{222}\text{Rn}$  measurements, there is also a rising diagonal line of events starting at  $\text{Ec} \sim 0 \text{ keV}$ ,  $\text{Ep} \sim 150 \text{ keV}$ . The slope varies between detectors, but the “peaks” along the line—allowing for a different energy scale and for non-linearity at low energies commonly observed for heavy charged particles in plastic scintillators (Knoll, 2000)—match the alpha energies in the  $^{222}\text{Rn}$  decay chain. We thus conclude that these events are alpha particles, generating a slightly different pulse shape (slower decay) than electrons or photons when interacting with the plastic scintillator. The PSA algorithms, in their current form, interpret the slower decay as a contribution of a slow CsI pulse and thus compute a component in Ec proportional to the pulse height. Because Rn is removed from the sample in Xe monitoring measurements to minimize interference in the 80-keV line, there should then be no significant interference from alpha particles either. On the other hand, it is also possible to modify the PSA algorithms to detect and remove alpha pulses from the recorded data, e.g., by shape-matching fits, measuring the fall time or additional sums over characteristic intervals in the pulse.
- In systems with separate beta and gamma detectors, Ec and Ep are measured separately, and thus are zero if the PMT output is below the trigger threshold. In the phoswich system, Ec and Ep are computed from a single measurement. For non-coincident events, Ec (or Ep) is thus *computed* as zero, but plus/minus a noise contribution, resulting in a distribution of events around the  $\text{Ec} = 0$  (or  $\text{Ep} = 0$ ) axis (see upper plots in Figure 2). The width of this distribution sets a lower bound to the energy of coincidence events to be distinguished from non-coincident events. The width is about 5–8 keV for Ec and about 20–30 keV for Ep, comparable to the trigger thresholds in systems with separate beta and gamma detectors. Using the PSA event categorization as plastic only, CsI only, or a combination, these events can be contracted to the axes, creating a spectrum similar to the one from systems with separate detectors (lower plots).

In monitoring applications, the samples of radioxenon collected are very small, so the background count rate of the detector has to be as small as possible. In a lead enclosure (the lead wall thickness is 2" with an additional 0.5" inner lining with oxygen-free high conductivity [OFHC] copper), we measure an overall rate of 3–8 counts/s for PW2–PW5, of which ~0.05–0.08 counts/s are coincidences. PW6 and PW7 show higher background rates (~10 counts/s, of which ~0.5 counts/s are in coincidence), which is currently being investigated. All detectors reject over 99% of radiation from an external  $^{137}\text{Cs}$  source as non-coincident. The background rate in the ARSA detector is ~30 counts/s, of which ~0.1 counts/s are coincident, i.e., the background is higher in the ARSA detector than in PW2–5; however, the ARSA detector uses a much larger NaI crystal.

To determine the coincidence detection efficiency, a series of measurements was performed with PW4 and PW5 using  $^{131\text{m}}\text{Xe}$ ,  $^{133}\text{Xe}$  and  $^{222}\text{Rn}$  at PNNL, and then analyzed following the procedure described in Cooper, 2007-2. We assume 98% beta efficiency (essentially the solid angle seen from the center of the Xe cell that is covered with aplastic scintillator, not a filling tube). The beta/gamma coincidence detection efficiency can be assumed to be (beta efficiency) times (gamma efficiency). From the  $^{131\text{m}}\text{Xe}$  data, we compute the gamma efficiency at 30 keV to be ~82%. Using this number and the  $^{133}\text{Xe}$  data, we compute the gamma efficiency at 80 keV to be ~65%. Using this number and the  $^{222}\text{Rn}$  data, we compute the gamma efficiency at 240 keV to be ~45–60%. The computed efficiencies have large uncertainties due to the limited statistics in the measurements and the methods to eliminate background and/or residual counts from previous sources, especially for the  $^{222}\text{Rn}$  measurements. However, numbers for PW4 and PW5 match to about 5% in most cases. Typical efficiencies measured on SAUNA detectors are ~75% gamma efficiency at 30 keV, ~85% gamma efficiency at 80 keV, ~65% gamma efficiency at 240 keV, but again it should be noted that measurement conditions vary. In particular, in the phoswich detector detection of low-energy X-rays is enhanced if they are in coincidence with beta particles since the latter creates a large PMT pulse that is easy to trigger on.

### Implementation of PSA Algorithms in On-Board DSP

As described in (Hennig, 2006-1), the signals from the phoswich detector are read out with a Pixie-4 module and processed with PSA algorithms to extract Ec and Ep, and to categorize events as CsI only (i.e., gamma only), plastic only (i.e., beta only) or both (i.e., beta/gamma coincidence). The algorithms use three quantities measured for each pulse, as illustrated in Figure 3: a) an overall pulse integral E computed from a trapezoidal filter with three energy sums, b) an integral P-B over the initial portion of the pulse, and c) the pulse rise time (RT). For CsI only (or plastic only) events, Ec (or Ep) is equal to E times a scaling factor, and E is proportional to P-B. The proportionality factor  $k_1$  (or  $k_2$ ) is a gain independent detector constant that can be determined in calibration measurements. For coincident

events, the factors  $k_1$  and  $k_2$  are used together with measured quantities  $E$  and  $P-B$  to compute  $E_c$  and  $E_p$  for each event. To categorize events as CsI only, plastic only, or both, the computed values of  $RT$ ,  $E_c$ , and  $E_p$  are compared against user defined thresholds.

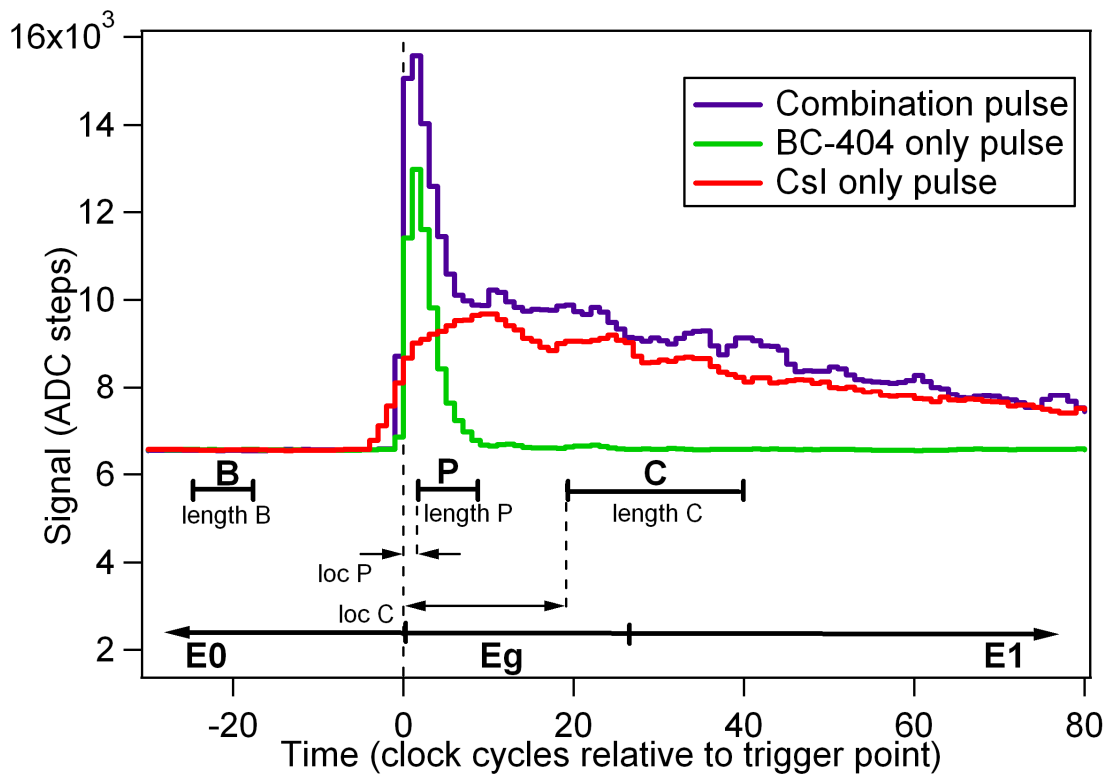


**Figure 3. Typical phoswich pulses and definition of filter sums in pulse shape analysis:** There is a sum  $B$  over the baseline region, a sum  $P$  over the initial part of the pulse, and a sum  $C$  over the later part of the pulse. To measure an overall integral over the pulse, the trapezoidal filter implemented in the readout electronics uses the energy filter sums  $E_0$ ,  $E_1$ , and  $E_g$  to compute the “energy”  $E$ . ( $P-B$ ) and  $E$  are used to compute  $E_p$  and  $E_c$ , the energy deposited in the BC-404 (plastic) and CsI scintillators. Also measured is the pulse  $RT$ .

In the past, for development purposes, the Pixie-4 measured  $E$  and acquired pulse waveforms, which are standard on-board pulse processing functions.  $P-B$  and  $RT$  were determined from the captured waveforms either by the on-board DSP with custom code or in offline analysis. Computation of  $E_c$  and  $E_p$ , event categorization, and accumulation of 1D and 2D spectra were always performed offline. Given the capabilities of the Pixie-4 and the desire to simplify and speed up operations on the host PC, all offline processing steps are now carried out in real time in the processing electronics, as illustrated in Figure 4. The standard functions of trigger detection, waveform capture, computation of energy filter sums, and pileup inspection are performed in field programmable gate arrays (FPGA) in parallel for four channels. For each channel that detected a valid pulse, the DSP uses the energy filter sums to compute  $E$ , analyzes the waveforms to compute  $P-B$  and  $RT$ , and computes  $E_p$  and  $E_c$ .  $RT$ ,  $E_p$ , and  $E_c$  are then compared to user-defined thresholds to categorize the event. Measured and computed quantities are stored in on-board memory as event-by-event list mode data. The energies are also binned into a 2D spectrum (256 x 256 bins) and six 1D spectra (up to 8K bins); three spectra for each  $E_c$  and  $E_p$  of a) all events, b) only non-coincident events and c) only coincident events. The memory can be read out through the PCI bus in fast block transfers over 80 Mbyte/s. In order to limit readout dead time, the list data memory is divided into two blocks so that data from one block can be read out while the data acquisition continues and stores data in the second block.

In the simplest mode of operation, it is only necessary to start and stop data acquisition in the Pixie-4 according to the sample preparation schedule, and periodically read out the spectrum memory to feed spectra into the isotope

analysis routines of the main system software. For more control and flexibility, the list data can be read as well and used to re-compute energies and/or re-bin spectra with custom binning parameters at a later time.

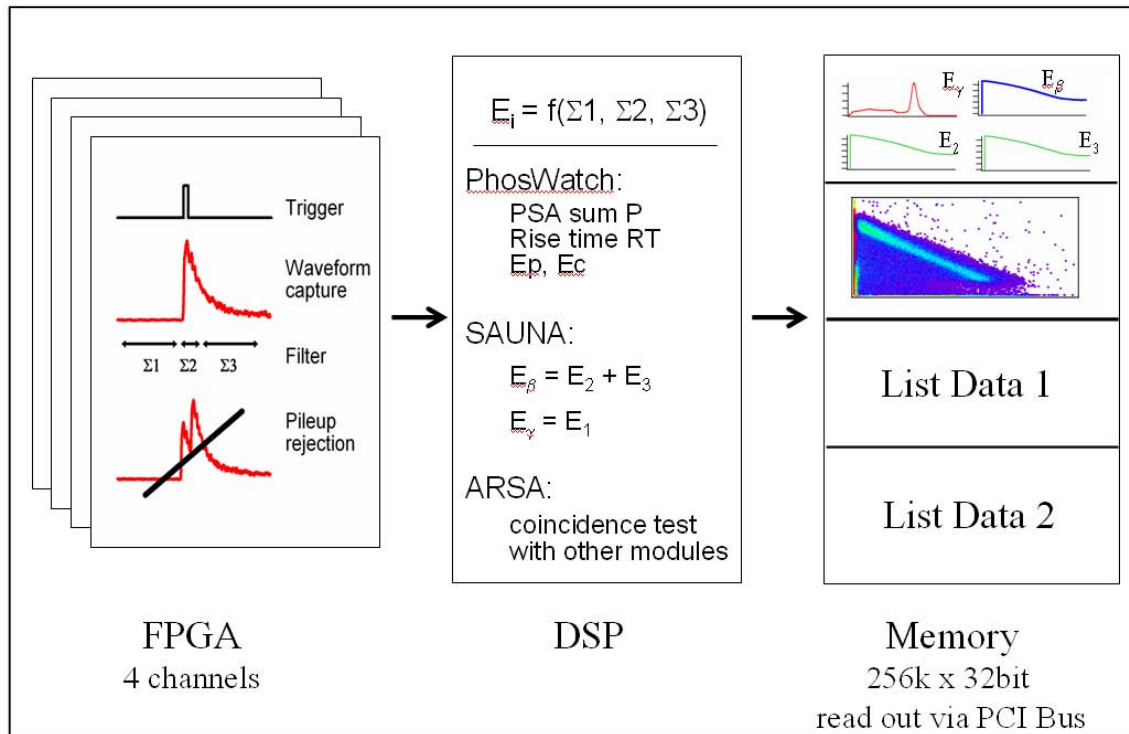


**Figure 4. Block diagram of processes in the Pixie-4. After digitization, pulses are detected in an FPGA that also computes energy filter sums. A DSP computes the energy  $E$ , analyzes the captured waveforms to compute PSA parameters, and computes  $E_\beta$  and  $E_\gamma$ . Energy histograms and list mode data are stored in on-board memory and can be read out to the host PC in fast block transfers.**

The Pixie-4, being multi-channel COTS readout electronics for a wide range of applications, can also be used in radioxenon detector systems with separate beta and gamma detectors (or even for systems like SPALAX (Fontaine, 2004) with a single high-resolution HPGe gamma detector). With the standard software, the Pixie-4 computes pulse heights and accumulates 1D spectra for each channel, providing sufficient data to build 2D spectra offline. Adapting some of the phoswich code customization, we also developed DSP code to better support ARSA or SAUNA detector systems. For example, to accommodate the two beta channels and one gamma channel in the SAUNA detector, the DSP code has been modified to sum the pulse heights from the two beta channels, and accumulate in its on-board memory 1D spectra of the beta sum energy, the individual beta energies, and the gamma energy, as well as a 2D beta/gamma spectrum. This code can also be used with the redesigned beta/gamma detector developed at PNNL (Cooper, 2007-1) which has one beta and one gamma channel. For the ARSA detector, having a total of 12 channels and thus requiring three Pixie-4 modules, an accumulation of 2D spectra in a single module is not possible, but the modules can share triggers and hit patterns to make accept/reject decisions based on the coincidence between channels and modules. This can be used to limit the acquisition to only events of interest and thus helps to better parse through data offline and compute beta and gamma sum energies from different channels.

The above changes in the on-board processing require no changes in the standard Pixie-4 driver library, except that the 2D spectrum data have to be interpreted differently from the standard 1D data format. Minor changes are required in the user interface to enter input parameters such as the length of P or event categorization thresholds (normally constants). These changes have been applied to the standard Pixie-4 user interface as an add-on software option, which also provides functions to display spectra, fit peaks in 1D spectra and sum regions of interest in the 2D spectrum.

### Programmable Coincidence Pulse Generator

The programmable coincidence pulse generator (“pulser”) shown in Figure 5 is a CompactPCI/PXI module meant to support monitoring and testing of the electronics for state of health during operation, and to allow the development or testing of acquisition and analysis software without the need for a detector and gas sources. It features four high-speed digital to analog converters (DAC) controlled by an FPGA that can be configured from a host PC through a PCI interface. This allows it to output four arbitrary pulse shapes, independent to each other or in coincidence, depending on the FPGA configuration and host control settings. The pulser can be placed in the signal path between detector and readout electronics, passing through the detector signal or switching to a test signal according to host control commands. In addition, the pulser generates eight simple exponential decay pulses, can fan out incoming signals to multiple channels, and provides general-purpose I/O for trigger signals. Several pulser modules can be operated synchronously for systems with a large channel count. The PCI interface is the same as in the Pixie-4 modules, allowing integrated host control software for both the Pixie-4 and the pulser.

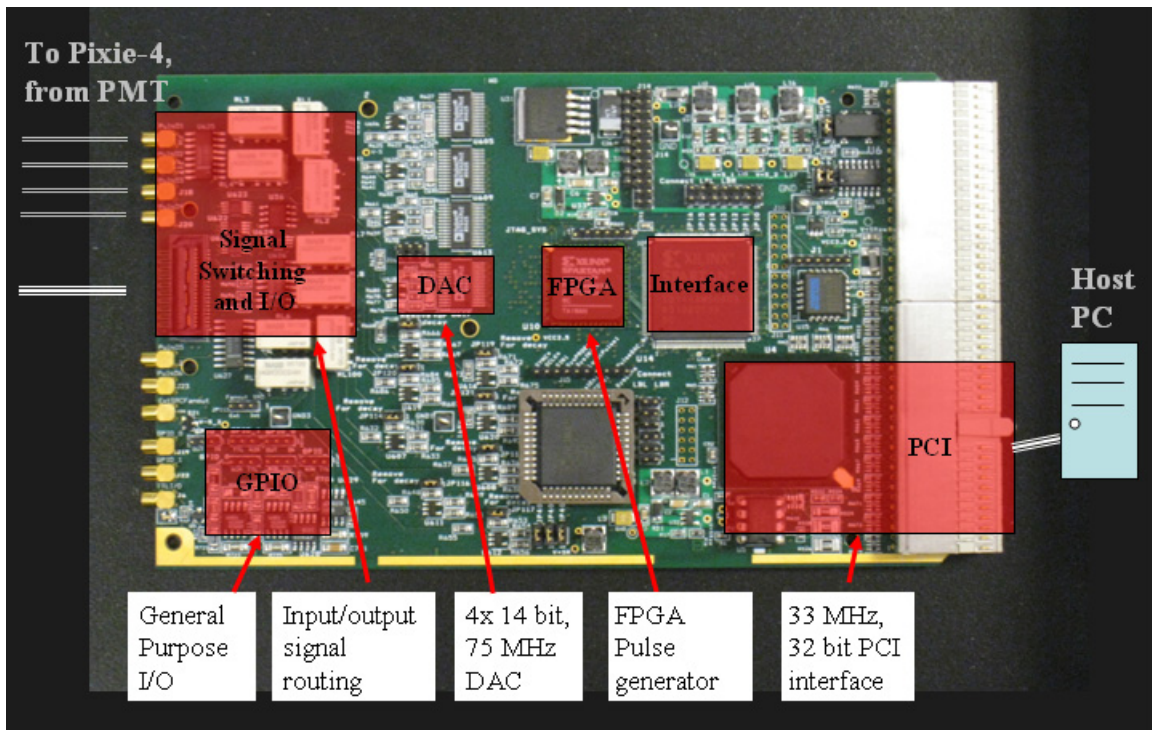


**Figure 5. Picture of the programmable coincidence pulse generator.** An FPGA, programmed through PCI interface, generates four arbitrary waveforms for high-speed DACs and up to eight simple exponential decay pulses. Through FPGA-controlled switches, either pulser signals or external detector signals can be output to the Pixie-4 readout electronics.

In a radioxenon monitoring system with a phoswich detector, one DAC channel of the pulser can thus be programmed to generate pulses with a fast and a slow component with varying amplitudes, simulating the phoswich detector response to exposure to radioxenon sources. During the acquisition, the host control software can periodically switch from detector signal to pulser test signal and verify that gains and threshold in the readout electronics are correct and that the test signal results are in the expected, reproducible test spectrum. In systems with separate beta and gamma detectors, several channels of the pulser can be programmed to generate coincident and non-coincident pulses from i) one or more plastic scintillators and ii) NaI or CsI scintillators, with pulse heights and count rates equivalent to the response to exposure to typical radioxenon sources.

### **CONCLUSIONS AND RECOMMENDATIONS**

In summary, we developed a COTS radioxenon detector unit, named “PhosWatch,” consisting of a phoswich detector, readout electronics, and PSA functions to detect beta/gamma coincidences. Of the six phoswich detectors manufactured so far, most achieve energy resolutions, background rates, and detection efficiencies comparable to the existing detectors. In particular, detectors using the R1307 PMT achieve an excellent resolution of ~7.3%

FWHM at 662 keV. The readout electronics consists of the DGF Pixie-4, a general purpose multi-channel spectrometer module with an on-board DSP performing the PSA functions to compute beta and gamma energies and detect coincidences. It accumulates 1D and 2D radioxenon spectra ready for isotope analysis and additionally records event-by-event list mode data for optional detailed offline analysis. We also developed a programmable coincidence pulse generator to support monitoring and testing of the electronics for state of health during operation. Several PhosWatch units are currently being beta-tested at radioxenon monitoring research laboratories.

The PhosWatch is intended as a drop-in replacement for existing detector units with separate beta and gamma channels. Requiring only a single PMT and electronics readout channel, the key benefit of the PhosWatch is its simpler setup, calibration and operation than the existing detector units. Some of the existing systems already use (or test use of) Pixie-4 modules as readout electronics. Since all phoswich-specific functions are contained in the DSP code, these systems can be upgraded with a PhosWatch without making changes in the system control software interfacing to the Pixie-4 C library except for formatting of spectrum data and definition of PSA input parameters (which are mostly constants). Future efforts will include the production of several additional PhosWatch units and their long term evaluation at radioxenon monitoring research laboratories, as well as updating and improving on-board PSA algorithms according to the experiences during evaluation.

#### **ACKNOWLEDGEMENTS**

We thank A. Ringbom for helpful information gleaned through private communications.

#### **REFERENCES**

- Cooper, M. W., J. I. McIntyre, T. W. Bowyer, A. J. Carman, J. C. Hayes, T. R. Heimbigner, C. W. Hubbard, L. Lidey, K. E. Litke, S. J. Morris, M.D. Ripplinger, R. Suarez, and R. Thompson (2007-1). Redesigned  $\beta$ - $\gamma$  radioxenon detector, *Nuclear Instruments and Methods in Physics Research A* 579, 426–430.
- Cooper, M.W., J. C. Hayes, T. R. Heimbigner, C. W. Hubbard, J. I. McIntyre, M. D. Ripplinger, and B. T. Schrom (2007-2). Automated QA/QC check for  $\beta$ - $\gamma$  coincidence detector, in *Proceedings of the 29th Monitoring Research Review: Ground Based Nuclear Explosion Monitoring Technologies*, LA-UR-07-5613, Vol. 2, pp. 739–746.
- Ely, J. H., C. E. Aalseth, J. C. Hayes, T. R. Heimbigner, J. I. McIntyre, H. S. Miley, M. E. Panisko, and M. Ripplinger (2003). Novel Beta-Gamma coincidence measurements using phoswich detectors, in *Proceedings of the 25th Seismic Research Review—Nuclear Explosion Monitoring: Building the Knowledge Base*, LA-UR-06-6029, Vol. 2, pp. 533–541.
- Farsoni, A.T., D.M. Hamby, K.D. Ropon, and S.E. Jones (2007). A two-channel phoswich detector for dual and triple coincidence measurements of radioxenon isotopes, in *Proceedings of the 29th Monitoring Research Review: Ground Based Nuclear Explosion Monitoring Technologies*, LA-UR-07-5613, pp. 747–756.
- Fontaine, J.-P., F. Pointurier, X. Blanchard and T. Taffary (2004). Atmospheric xenon radioactive isotope monitoring, *Journal of Environmental Radioactivity* 72: 129–135.
- Hennig, W., H.Tan, W. K. Warburton, and J. I. McIntyre (2006-1). Single channel beta-gamma coincidence detection of radioactive Xenon using digital pulse shape analysis of phoswich detector signals, *IEEE Transactions on Nuclear Science* 53: (2) p. 620.
- Hennig, W., H.Tan, A. Fallu-Labruyere, W. K. Warburton, J. I. McIntyre and A. Gleyzer (2006-2). Design of a phoswich well detector for radioxenon monitoring, in *Proceedings of the 28th Seismic Research Review: Ground Based Nuclear Explosion Monitoring Technologies*, LA-UR-06-5471, Vol. 2, pp. 801–810.
- Hennig, W., H.Tan, A. Fallu-Labruyere, W. K. Warburton, J. I. McIntyre, and A. Gleyzer (2007-1). Characterization of phoswich well detectors for radioxenon monitoring, in *Proceedings of the 29th Monitoring Research Review: Ground Based Nuclear Explosion Monitoring Technologies*, LA-UR-07-5613, pp. 757–763.

## **2008 Monitoring Research Review: Ground-Based Nuclear Explosion Monitoring Technologies**

Hennig, W., Y.X. Chu, H.Tan, A. Fallu-Labruyere, W. K. Warburton, and R. Grzywacz (2007-2). The DGF Pixie-4 spectrometer – Compact Digital Readout Electronics for HPGe Clover Detectors, *Nuclear Instruments and Methods in Physics Research B* 263, 175-178.

Knoll, G. F. (2000) *Radiation Detection and Measurement*, J Wiley & Sons, Inc. Chapter 8.

Reeder, P. L., T. W. Bowyer, and R. W. Perkins, (1998). Beta-gamma counting system for Xe fission products, *Journal of Radioanalytical and Nuclear Chemistry* 235: (1–2), 89–94.

Reeder, P. L., T. W. Bowyer, J. I. McIntyre, W. K. Pitts, A. Ringbom, and C. Johansson (2004). Gain calibration of coincidence spectrometer for automated radioxenon analysis., *Nuclear Instruments and Methods in Physics Research A* 521: 586–599.

Ringbom, A., T. Larson, A. Axelson, K. Elmgren, and C. Johansson (2003). SAUNA—a system for automatic sampling, processing and analysis of radioactive xenon, *Nuclear Instruments and Methods in Physics Research A* 508: 542–553.